IEEE Access
Multidisciplinary | Rapid Review | Open Access Journal

Received March 5, 2019, accepted March 25, 2019, date of publication April 1, 2019, date of current version April 15, 2019.

Digital Object Identifier 10.1109/ACCESS.2019.2908407

Joint Trajectory and Power Design for UAV-Enabled Secure Communications With No-Fly Zone Constraints

YING GAO[1,2], HONGYING TANG[1], BAOQING LI[1], AND XIAOBING YUAN[1]

[1]Science and Technology on Microsystem Laboratory, Shanghai Institute of Microsystem and Information Technology, Chinese Academy of Sciences, Shanghai 201800, China

[2]University of Chinese Academy of Sciences, Beijing 100049, China

Corresponding author: Baoqing Li (sinoiot@mail.sim.ac.cn)

This work was supported in part by the Shanghai Natural Science Foundation under Grant 17ZR1428900, and in part by the Foundation of the Key Laboratory of National Defense for Science and Technology of China under Grant 6142804010304.

ABSTRACT Unmanned aerial vehicles (UAVs) have attracted growing interest in wireless communications due to their several superiorities, such as highly controllable mobility, favorable communication links with the ground, on-demand deployment, and low cost. This paper investigates a UAV-ground communication system, where a UAV is dispatched to send classified information to a legitimate user in the presence of an eavesdropper on the ground while simultaneously avoiding flying over the no-fly zones (NFZs). We aim to maximize the average secrecy rate of the system by jointly optimizing the UAV's trajectory and transmit power over a given flight period under the practical constraints on the UAV's maximum speed, the initial and final locations, avoidance of NFZs, as well as the transmit power. Although the existing works have studied a similar secrecy rate maximization problem, they all rely on general-purpose solvers, which leads to considerably high computational complexity. To address this issue, we propose an efficient algorithm by applying the techniques of alternating optimization (AO) and successive convex approximation (SCA) to obtain a suboptimal solution and utilizing the alternating directional method of multipliers (ADMM) under the SCA framework to realize low-complex implementation. The simulation results demonstrate the superior computational efficiency of our proposed algorithm and show the impact of NFZs on the system.

INDEX TERMS Unmanned aerial vehicles (UAVs), physical layer security, no-fly zone (NFZ) constraints, joint trajectory and power design, alternating directional method of multipliers (ADMM).

I. INTRODUCTION

The unmanned aerial vehicle (UAV) has recently emerged as a promising technique in military and civilian domains, such as surveying and mapping, surveillance and monitoring, power patrol inspection, etc. Several benefits of UAVs, such as high flexibility, the ability of on-demand deployment and low operational cost, are attractive to wireless service providers [1]. Specifically, as a high possibility exists of having line-of-sight (LoS) links with ground users, UAVs possess dependable air-to-ground channels and hence can be deployed as aerial base stations (BSs) to enhance the existing wireless communication networks' capacity, or provide temporary service in disaster-affected areas. Moreover, UAV-aided wireless networks can achieve performance enhancement via cautious trajectory design, besides conventional communication resource assignment.

The above advantages have inspired a proliferation of researches on UAV-aided communications. Earlier studies mainly focus on the placement optimization of UAVs as aerial quasi-static BSs [2]–[4], where the UAVs are employed to serve a group of ground users. To fully leverage the UAV's mobility, people turn their attention to the dynamic trajectory design. Extensive research efforts have been devoted to the trajectory optimization of UAVs in multiple access systems [5]–[8], broadcast channels [9], relaying systems [10], [11], energy-efficient communications [12], [13], multi-UAV networks [14], and mobile-edge computing systems [15]–[17]. However, due to the broadcast nature of LoS channels, it is difficult to guarantee the confidentiality of

The associate editor coordinating the review of this manuscript and approving it for publication was Yue Cao.

2169-3536 © 2019 IEEE. Translations and content mining are permitted for academic research only.
Personal use is also permitted, but republication/redistribution requires IEEE permission.
See http://www.ieee.org/publications_standards/publications/rights/index.html for more information.

UAV-ground communications since sent messages are more likely to be divulged to the potential ground eavesdroppers.

A. RELATED WORK AND MOTIVATION

Recently, as an alternative to conventional cryptographic methods, physical (PHY) layer security has drawn growing attention in wireless communication fields. There have been prior works on UAV-assisted secure communications, where the secrecy rate is regarded as the performance metric. Reference [18] investigates both the downlink and uplink communication systems, and proposes an efficient algorithm to maximize the average secrecy rate by jointly optimizing the UAV trajectory and transmit power. Considering a more practical scenario where the locations of multiple eavesdroppers are imperfectly known to the UAV, the authors in [19] propose a joint design algorithm of robust trajectory and transmit power of the UAV to maximize the worst-case secrecy rate of the system. For a UAV-aided mobile relaying system, the authors in [20] optimize the transmit power of the source/relay to improve the PHY security of the system, assuming the UAV flies unidirectionally from source to destination at a constant altitude and velocity. Following [20], reference [21] considers a joint source/relay transmit power and trajectory design problem for a UAV-enabled relaying network, and shows that the trajectory optimization is vital for secrecy enhancement. In [22], the UAV works as a friendly jammer to secure the ground wiretap channel, rather than a legitimate transmitter. The authors in [23] consider a novel UAV-aided secure communication system with cooperative jamming, where a UAV communicates with multiple ground users in a time division multiple access (TDMA) manner while a collaborative UAV sends jamming signal to defend against potential overhearing. A joint user scheduling, trajectory and transmit power optimization algorithm is proposed to maximize the minimum secrecy rate among the users. Reference [24] formulates an optimization problem similar to that in [23] for the frequency division multiple access (FDMA) systems, while taking into account the collision avoidance in the trajectories design of the UAV transmitter and jammer. In [25], the authors investigate the worst-case secrecy rate maximization by assuming that the UAV transmitter and jammer have incomplete knowledge of the single eavesdropper's location. Besides, the authors in [26] propose a novel scheme via jointly optimizing the UAV trajectory and time scheduling to guarantee the security of a UAV-relayed wireless network with local caching. A recent work [27] studies an energy efficiency maximization problem for a secure UAV-enabled orthogonal frequency division multiple access (OFDMA) network with multiple legitimate users and a potential eavesdropper located at an uncertain region.

A conventional method widely adopted in the above works is to combine the techniques of alternating optimization (AO) and successive convex approximation (SCA), which is called SCA-AO in the following content. Specially, AO technique optimizes trajectory variables and communication resource variables alternately and iteratively, while SCA framework addresses the non-convexity of subproblems by applying the first-order Taylor expansion. However, due to dependency on general-purpose solvers such as CVX [28], SCA-AO is too time-consuming. Even worse, its complexity increases noticeably as the problem scale goes up. As a powerful first-order approach, the alternating directional method of multipliers (ADMM) [29] offers a solution to reduce the computational complexity, and has successfully applied to large-scale problems for beamforming design and resource allocation in various wireless networks. Decentralized algorithms based on the combination of the SCA framework and the ADMM approach are developed in [30] for the energy efficiency fairness optimization problem in a multicell multiuser multiple-input single-output downlink system. The authors in [31] consider the multi-group multicast beamforming design problem in large-scale wireless systems, and propose a low-complexity high-performance algorithm by exploiting the advantages of the ADMM method together with the convex-concave procedure (CCP) principle. It is demonstrated in their work that the ADMM-based algorithm has a great superiority in computational efficiency.

It's worth mentioning that although literatures mentioned above on UAV trajectory design have considered many mobility constraints, such as flying speed, initial/final location, collision avoidance and so on, they pay little attention to the geographic restrictions on trajectory planning. For instance, there are some no-fly zones (NFZs) where UAVs are banned from flying for threat avoidance or policy factors. Currently, limited researches have been done on UAV trajectory optimization considering the NFZ constraints. Reference [32] develops a safe-distance-based strategy for NFZ avoidance in the formation control of multiple UAVs. In [33], a path planning module is presented to calculate quasi-optimal trajectories for UAVs in the context of military operations with multiple NFZs. As far as we know, the authors in [34] firstly take the NFZ constraints into account in joint trajectory and resource allocation design for UAV-enabled air-to-ground communication systems. Up to now, no efforts have been made to the study of secure UAV communications with the NFZ constraints.

B. CONTRIBUTIONS

Motivated by the analyses above, we study in this paper a downlink secure transmission scenario as shown in Fig.1, where a UAV delivers secret messages to a legitimate receiver in the presence of an on-ground eavesdropper. Meanwhile, the UAV is prohibited from flying over the NFZs. We formulate a joint UAV trajectory and power optimization problem to maximize the achievable average secrecy rate over a finite flight period, while guaranteeing the UAV's maximum speed, the initial and final locations, the NFZ constraints, as well as the transmit power constraints. Specifically, the main technical novelty and research findings of this paper are summarized as follows.

- To our best knowledge, this paper is the first work that considers NFZ constraints in secure

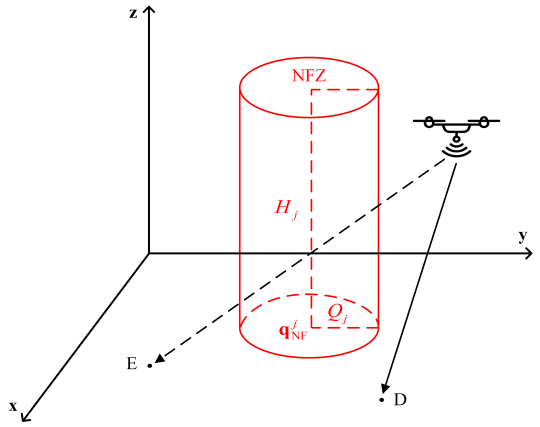


FIGURE 1. A UAV-enabled secure communication system with the restriction of a no-fly zone.

UAV communications, which is more practical in comparison with the similar work without NFZ consideration [18].

- The formulated problem is non-convex due to the coupling of power and trajectory variables, and hence there is no general method to obtain the globally optimal solution. We thus propose an efficient algorithm via the AO technique to obtain a suboptimal solution, which alternately optimizes transmit power variables and trajectory variables in an iterative manner until convergence.
- The trajectory optimization subproblem with fixed power control is still challenging to solve due to its non-convexity. We thus apply the SCA technique to transform the non-convex subproblem into a convex approximate one in each iteration, with fewer slack variables compared to [18]. Furthermore, to reduce the computational complexity, each resulting convex approximate subproblem is then reformulated as an equivalent ADMM form, which enables closed-form solutions in each updating step.
- Numerical results show that our proposed ADMM-based iterative algorithm achieves the same favorable performance as the CVX-based method SCA-AO, with dramatically reduced computation time. Besides, compared to the benchmark scheme without transmit power control, the proposed algorithm can improve the security performance. Simulation results provide helpful insights for the impact of NFZs on secure UAV communications as well.

Different from those similar works solved by general-purpose solvers, we leverage the ADMM approach to realize low-complex implementation. It is worth pointing out that although we investigate a downlink secure transmission scenario, our proposed algorithm can be modified easily to work for the secrecy rate maximization problems in uplink UAV communication systems, or in the case that the UAV is employed as a cooperative jammer to secure the ground wireless communication [22]. We also note that the authors in [27] solve their considered convex optimization subproblem for user scheduling and power control by adopting the dual decomposition method, rather than general-purpose solvers. However, for our considered convex approximate subproblem for trajectory optimization, this method has no advantage over our proposed ADMM-based algorithm. If the dual decomposition method is applied in our case, updating steps can be carried out neither separately in parallel for each trajectory variable, nor in closed-form solutions, since trajectory variables are coupled between neighbor time slots in the constraints. Our proposed ADMM-based algorithm realizes the decoupling of trajectory variables between neighbor time slots, and enables closed-form solutions in each updating step. Thus, there is no doubt that our proposed algorithm is more time-efficient than the dual decomposition method.

C. ORGANIZATION AND NOTATIONS

The rest of this paper is organized as follows. Section II introduces the system model for a UAV-enabled secure communication network and formulates the average secrecy rate maximization problem. In section III, we propose a low-complexity ADMM-based iterative algorithm for the considered problem. Section IV provides numerical results to demonstrate the efficacy of the proposed algorithm. Finally, we conclude the paper in Section V.

Notations: In this paper, scalars are denoted by italic letters, while column vectors and matrices are denoted by boldface lower-case and upper-case letters, respectively. $\|\cdot\|$ denotes the Euclidean norm of a vector, and the superscript $(\cdot)^T$ represents the transpose. $\mathbf{I}_K$ is the $K \times K$ identity matrix; $\mathbf{0}_K$ is the K-dimensional all-zero vector. $\mathbb{R}^{N\times 1}$ denotes the space of N-dimensional real-valued vector. Notation $\otimes$ denotes the Kronecker product.

II. SYSTEM MODEL AND PROBLEM FORMULATION

A. SYSTEM MODEL

As shown in Fig.1, we consider a downlink transmission scenario where a UAV transmits private information to a legitimate receiver D in the presence of an eavesdropper E, while simultaneously avoiding flying over the NFZs. Both D and E are assumed at fixed locations on the ground which are known to the UAV.

Without loss of generality, we consider a three-dimensional (3D) Cartesian coordinate system with node i's horizontal coordinate denoted by $\mathbf{w}_i = [x_i, y_i]^T \in \mathbb{R}^{2\times 1}$, $i \in \{\mathrm{D}, \mathrm{E}\}$. To avoid unnecessary energy consumption on aircraft ascending or descending, the UAV is assumed to fly horizontally at a fixed altitude H in meter (m). The results in this paper can be readily extended to the case with varying altitude as well. The initial and final locations of the UAV are predetermined, which are denoted as $\mathbf{q}_0 = [x_0, y_0]^T$ and $\mathbf{q}_{\mathrm{F}} = [x_{\mathrm{F}}, y_{\mathrm{F}}]^T$, respectively. Here, T in second (s) denotes the flight period of the UAV. For convenience, we divide T into N time slots with each slot duration $\delta_t = T/N$, which is adequately small such that the UAV's location can be

regarded as almost unchanged within each time slot [35]. Thus, the UAV's horizontal trajectory over the flight period T can be approximated by the sequence $\mathbf{q}[n] = [x[n], y[n]]^T$, $n = 1, \cdots, N$. Furthermore, we assume that there are J non-overlapped NFZs of sparse distribution where the UAV is strictly prohibited to fly. The NFZ $j \in \{1, \cdots, J\}$ is defined as a cylindrical region with a finite height H_j in m, $H \leq H_j, \forall j$. Denote the horizontal coordinate center and radius of each NFZ j by $\mathbf{q}_{\mathrm{NF}}^j = [x_{\mathrm{NF}}^j, y_{\mathrm{NF}}^j]^T$ and $Q_j, \forall j$, respectively. Subject to the maximum speed constraints and NFZ constraints, the UAV trajectory should satisfy

$$\|\mathbf{q}[1] - \mathbf{q}_0\|^2 \leq S_{\max}^2, \tag{1a}$$
$$\|\mathbf{q}[n+1] - \mathbf{q}[n]\|^2 \leq S_{\max}^2, \quad n = 1, \cdots, N-1, \tag{1b}$$
$$\|\mathbf{q}_{\mathrm{F}} - \mathbf{q}[N]\|^2 \leq S_{\max}^2, \tag{1c}$$
$$\|\mathbf{q}[n] - \mathbf{q}_{\mathrm{NF}}^j\|^2 \geq Q_j^2, \quad \forall n, j, \tag{1d}$$

where $S_{\max} \triangleq V_{\max}\delta_t$ is the maximum horizontal distance that the UAV can travel within one time slot on the assumption of maximum speed $V_{\max}$ in meter/second (m/s).

As shown in the measurement results [1], [36], [37], the air-to-ground communication channels are primarily dominated by LoS link. Following the free-space path loss model normally adopted in prior literatures on UAV-aided communications, the channel power gain from the UAV to node $i \in \{\mathrm{D}, \mathrm{E}\}$ in time slot n can be expressed as

$$h_i[n] = \beta_0\, d_i^{-2}[n] = \frac{\beta_0}{H^2 + \|\mathbf{q}[n] - \mathbf{w}_i\|^2}, \quad \forall n, \tag{2}$$

where $d_i[n] = \sqrt{H^2 + \|\mathbf{q}[n] - \mathbf{w}_i\|^2}$ is the link distance between the UAV and node i in time slot n, and β_0 denotes the channel power gain at the reference distance of 1 m, whose value is dependent on the antenna gain, the carrier frequency, etc.

The transmit power of the UAV in time slot n is denoted by $p[n]$, which is subject to the following constraints

$$\frac{1}{N}\sum_{n=1}^{N} p[n] \leq \bar{P}, \tag{3a}$$
$$0 \leq p[n] \leq P_{\mathrm{peak}}, \ \forall n, \tag{3b}$$

with $\bar{P}$ and P_{peak} denoting the average power and the peak power, respectively. Accordingly, the achievable rate from the UAV to node $i \in \{\mathrm{D}, \mathrm{E}\}$ in time slot n, denoted by $R_i[n]$ in bits/second/Hertz (bps/Hz), can be expressed as

$$R_i[n] = \log_2\left(1 + \frac{\gamma_0 p\,[n]}{H^2 + \|\mathbf{q}\,[n] - \mathbf{w}_i\|^2}\right), \quad \forall n, \tag{4}$$

where $\gamma_0 = \frac{\beta_0}{\sigma^2}$ represents the reference signal-to-noise ratio (SNR) and σ^2 denotes the independent Gaussian noise power at D or E. As a consequence, the average achievable secrecy rate from the UAV to the legitimate receiver D over N time slots in bps/Hz is given by

$$R_{\mathrm{sec}} = \frac{1}{N}\sum_{n=1}^{N}\Big[R_{\mathrm{D}}[n] - R_{\mathrm{E}}[n]\Big]^+, \tag{5}$$

where $[x]^+ \triangleq \max(x, 0)$. The operator $[\cdot]^+$ in (5) makes the function non-smooth at zero value.

B. PROBLEM FORMULATION

For notational convenience, let $\mathbf{q} \triangleq \{\mathbf{q}[n], \forall n\}$ and $\mathbf{p} \triangleq \{p[n], \forall n\}$. We aim to maximize the achievable average secrecy rate in (5) via jointly optimizing the UAV's trajectory $\mathbf{q}$ and transmit power $\mathbf{p}$ over all time slots, while taking into account the maximum speed constraints and NFZ constraints in (1) and transmit power constraints in (3). The problem of our interest can be formulated as

$$\max_{\mathbf{q},\mathbf{p}} \frac{1}{N}\sum_{n=1}^{N}\left[\log_2\left(1 + \frac{\gamma_0 p\,[n]}{H^2 + \|\mathbf{q}\,[n] - \mathbf{w}_{\mathrm{D}}\|^2}\right) - \log_2\left(1 + \frac{\gamma_0 p\,[n]}{H^2 + \|\mathbf{q}\,[n] - \mathbf{w}_{\mathrm{E}}\|^2}\right)\right]$$
$$\text{s.t. (1), (3)}, \tag{6}$$

where the operator $[\cdot]^+$ has been ignored, since according to [18], a non-negative secrecy rate at each time slot can always be achieved by controlling the transmit power of the UAV. Notice that although smooth, problem (6) is still non-convex and challenging to solve.

III. PROPOSED SOLUTION

In this section, we propose a low-complexity ADMM-based iterative algorithm for solving problem (6). Specifically, problem (6) is partitioned into two subproblems, namely power optimization with fixed trajectory and trajectory optimization with fixed power control, which are solved alternately in an iterative manner until convergence is achieved.

A. POWER OPTIMIZATION

For any given UAV trajectory $\mathbf{q}$, problem (6) can be written as

$$\max_{\mathbf{p}} \frac{1}{N}\sum_{n=1}^{N}\left[\log_2\left(1 + a_n p[n]\right) - \log_2\left(1 + b_n p[n]\right)\right]$$
$$\text{s.t. (3)}, \tag{7}$$

where

$$a_n = \frac{\gamma_0}{H^2 + \|\mathbf{q}\,[n] - \mathbf{w}_{\mathrm{D}}\|^2}, \quad b_n = \frac{\gamma_0}{H^2 + \|\mathbf{q}\,[n] - \mathbf{w}_{\mathrm{E}}\|^2}. \tag{8}$$

Although problem (7) is non-convex with respect to $\mathbf{p}$, its optimal solution can be obtained as shown in [38]

$$p^*\,[n] = \begin{cases} \min\left(\left[\hat{p}\,[n]\,\right]^+, P_{\mathrm{peak}}\right) & a_n > b_n, \\ 0 & a_n \leqslant b_n, \end{cases} \tag{9}$$

where

$$\hat{p}\,[n] = \sqrt{\left(\frac{1}{2b_n} - \frac{1}{2a_n}\right)^2 + \frac{1}{\lambda \ln 2}\left(\frac{1}{b_n} - \frac{1}{a_n}\right)} - \frac{1}{2b_n} - \frac{1}{2a_n}. \tag{10}$$

In (10), λ is a non-negative parameter that ensures constraint (3a), which can be found efficiently by bisection search [28].

B. UAV TRAJECTORY OPTIMIZATION

Given any feasible power allocation $\mathbf{p}$, problem (6) is simplified into the following problem for optimizing the UAV trajectory $\mathbf{q}$ only, i.e.,

$$\max_{\mathbf{q}} \frac{1}{N}\sum_{n=1}^{N}\left[\log_2\left(1+\frac{\gamma[n]}{H^2+\|\mathbf{q}[n]-\mathbf{w}_{\mathrm{D}}\|^2}\right) - \log_2\left(1+\frac{\gamma[n]}{H^2+\|\mathbf{q}[n]-\mathbf{w}_{\mathrm{E}}\|^2}\right)\right] \quad \text{s.t. (1)}, \tag{11}$$

where $\gamma[n] \triangleq \gamma_0 p[n]$. Note that the problem (11) is non-convex due to the non-convexity of the objective function and constraint (1d). In general, it cannot be solved efficiently.

1) SCA FRAMEWORK

By introducing the slack variables $\mathbf{t} = [t[1], \cdots, t[n]]^T$, we can reformulate problem (11) as

$$\max_{\mathbf{q},\mathbf{t}} \frac{1}{N}\sum_{n=1}^{N}\left[\log_2\left(1+\frac{\gamma[n]}{H^2+\|\mathbf{q}[n]-\mathbf{w}_{\mathrm{D}}\|^2}\right) - \log_2\left(1+\frac{\gamma[n]}{t[n]}\right)\right] \tag{12a}$$

$$\text{s.t. } t[n] \le H^2+\|\mathbf{q}[n]-\mathbf{w}_{\mathrm{E}}\|^2, \quad \forall n, \tag{12b}$$

$$(1).$$

It is easy to prove that constraint (12b) holds with equality at the optimal point of problem (12), since otherwise the objective value could be further improved as $t[n]$ increases without violating constraint (12b). However, problem (12) is still non-convex due to the term $\log_2\left(1+\frac{\gamma[n]}{H^2+\|\mathbf{q}[n]-\mathbf{w}_{\mathrm{D}}\|^2}\right)$ in the objective function and constraints (12b) and (1d). To tackle the non-convexity, we adopt the SCA technique to obtain a converged approximate solution of problem (12) in an iterative way. Specially, $\{\mathbf{q}^r[n], \forall n\}$ stands for the given UAV trajectory in the r-th iteration. Note that since $\log_2\left(1+\frac{\gamma[n]}{H^2+\|\mathbf{q}[n]-\mathbf{w}_{\mathrm{D}}\|^2}\right)$ is a convex function with respect to $\|\mathbf{q}[n]-\mathbf{w}_{\mathrm{D}}\|^2$, we can obtain the following convex lower bound for it as in [7], i.e.,

$$\log_2\left(1+\frac{\gamma_{[n]}}{H^2+\|\mathbf{q}[n]-\mathbf{w}_{\mathrm{D}}\|^2}\right) \ge -A^r[n](\|\mathbf{q}[n]-\mathbf{w}_{\mathrm{D}}\|^2-\|\mathbf{q}^r[n]-\mathbf{w}_{\mathrm{D}}\|^2)+B^r[n], \tag{13}$$

where

$$A^r[n] = \frac{\gamma[n]\log_2 e}{(H^2+\|\mathbf{q}^r[n]-\mathbf{w}_{\mathrm{D}}\|^2)(H^2+\|\mathbf{q}^r[n]-\mathbf{w}_{\mathrm{D}}\|^2+\gamma[n])}, \tag{14}$$

$$B^r[n] = \log_2\left(1+\frac{\gamma[n]}{H^2+\|\mathbf{q}^r[n]-\mathbf{w}_{\mathrm{D}}\|^2}\right). \tag{15}$$

In constraint (12b), since $\|\mathbf{q}[n]-\mathbf{w}_{\mathrm{E}}\|^2$ is convex with respect to $\mathbf{q}[n]$, its first-order Taylor expansion at the given point $\mathbf{q}^r[n]$ is a global over-estimator, i.e.,

$$\|\mathbf{q}[n]-\mathbf{w}_{\mathrm{E}}\|^2 \ge \|\mathbf{q}^r[n]-\mathbf{w}_{\mathrm{E}}\|^2+2\left(\mathbf{q}^r[n]-\mathbf{w}_{\mathrm{E}}\right)^T \times\left(\mathbf{q}[n]-\mathbf{q}^r[n]\right) \triangleq D_E^r[n]. \tag{16}$$

Similarly, we obtain the following inequality in constraint (1d)

$$\left\|\mathbf{q}[n]-\mathbf{q}_{\mathrm{NF}}^j\right\|^2 \ge \left\|\mathbf{q}^r[n]-\mathbf{q}_{\mathrm{NF}}^j\right\|^2+2\left(\mathbf{q}^r[n]-\mathbf{q}_{\mathrm{NF}}^j\right)^T \times\left(\mathbf{q}[n]-\mathbf{q}^r[n]\right) \triangleq D_{\mathrm{NF}}^{j^r}[n], \quad \forall j. \tag{17}$$

With any given local point $\{\mathbf{q}^r[n], \forall n\}$ in the r-th iteration as well as the lower bounds in (13), (16) and (17), problem (12) is approximated as

$$\min_{\mathbf{q},\mathbf{t}} \frac{1}{N}\sum_{n=1}^{N}\left[A^r[n]\|\mathbf{q}[n]-\mathbf{w}_{\mathrm{D}}\|^2 + \log_2\left(1+\frac{\gamma[n]}{t[n]}\right)\right] \tag{18a}$$

$$\text{s.t. } t[n] \le H^2+D_E^r[n], \ \forall n, \tag{18b}$$

$$Q_j^2 \le D_{\mathrm{NF}}^{j^r}[n], \quad \forall n, j, \tag{18c}$$

$$(1a), (1b), (1c).$$

Since the objective function is convex, (18b) and (18c) are all linear constraints while (1a)-(1c) are all convex quadratic constraints, (18) is a convex optimization problem that can be efficiently solved by general-purpose solvers such as CVX. Since CVX invokes the interior-point method to solve convex optimization problems, the complexity of solving problem (18) is $\mathcal{O}\left(N^{\frac{7}{2}}J^{\frac{3}{2}}\right)$ based on the analyses in [7], [39], where N and J are the number of time slots and NFZs, respectively. Obviously, this leads to a fairly high computational complexity, especially in the case of rather long flight period.

Remark 1: In comparison with the existing work in [18], the main novelty of our proposed SCA framework is reducing the number of introduced slack variables by N, contributing to an easier reformulation of the framework as an ADMM one, as this paper shows later.

2) ADMM-BASED ALGORITHM

To reduce the computational complexity, we propose an ADMM-based algorithm to solve problem (18), whose each updating step only requires some multiplications and additions instead of general-purpose solvers. Towards this end, we introduce $\mathbf{m}[n]$ as the copy of the original trajectory vector $\mathbf{q}[n]$ at node D and E. For ease of notation, we define $\mathbf{m} \triangleq \left[\mathbf{m}^T[1], \cdots, \mathbf{m}^T[n]\right]^T \in \mathbb{R}^{2N\times 1}$. Hence, problem (18)

can be equivalently expressed as

$$\min_{\mathbf{q},\mathbf{t},\mathbf{m}} \frac{1}{N}\sum_{n=1}^{N}\Bigg[A^r[n]\|\mathbf{m}[n]-\mathbf{w}_{\mathrm{D}}\|^2 + \log_2\left(1+\frac{\gamma[n]}{t[n]}\right)\Bigg] \tag{19a}$$

$$\text{s.t. } \mathbf{m}=\mathbf{q}, \tag{19b}$$

$$(\mathbf{m},\mathbf{t})\in\mathcal{S},$$

$$\text{(1a), (1b), (1c), (18c)}, \tag{19c}$$

where the feasible region of $(\mathbf{m},\mathbf{t})$ is denoted by

$$\mathcal{S}=\{\,\mathbf{m},\mathbf{t}\mid t[n]\le H^2+\|\mathbf{q}^r[n]-\mathbf{w}_{\mathrm{E}}\|^2+2\left(\mathbf{q}^r[n]-\mathbf{w}_{\mathrm{E}}\right)^T \times\left(\mathbf{m}[n]-\mathbf{q}^r[n]\right),\quad \forall n\,\}. \tag{20}$$

However, the constraints (1a)-(1c) are still coupled between neighbor time slots. To overcome this difficulty, we define $\mathbf{z}_1\triangleq\mathbf{q}[1]-\mathbf{q}_0$, $\mathbf{z}_n\triangleq\mathbf{q}[n]-\mathbf{q}[n-1], n=2,\cdots,N$, $\mathbf{z}_{N+1}\triangleq\mathbf{q}_{\mathrm{F}}-\mathbf{q}[N]$, $\mathbf{z}\triangleq[\mathbf{z}_1^T,\cdots,\mathbf{z}_{N+1}^T]^T\in\mathbb{R}^{2(N+1)\times1}$ and $\mathbf{v}\triangleq\left[\mathbf{q}_0^T,\mathbf{0}_{2(N-1)}^T,-\mathbf{q}_{\mathrm{F}}^T\right]^T\in\mathbb{R}^{2(N+1)\times1}$. Then constraints (1a)-(1c) can be compactly expressed as $\mathbf{D}\mathbf{q}-\mathbf{v}=\mathbf{z},\mathbf{z}_n\in\mathcal{Z}$, $\forall n$, where $\mathcal{Z}\triangleq\{\mathbf{z}_n\|\mathbf{z}_n\|\le S_{\max}\}$ is the feasible region of $\mathbf{z}_n$ and $\mathbf{D}=\mathbf{D}_0\otimes\mathbf{I}_2\in\mathbb{R}^{2(N+1)\times2N}$,

$$\mathbf{D}_0=\begin{bmatrix}1&0&0&\cdots&0\\-1&1&0&\cdots&0\\0&-1&1&\cdots&0\\\vdots&\vdots&\vdots&\ddots&\vdots\\0&0&0&\cdots&1\\0&0&0&\cdots&-1\end{bmatrix}\in\mathbb{R}^{(N+1)\times N}.$$

Similarly, we define $\mathbf{h}_n\triangleq\mathbf{q}[n],\forall n$ and $\mathbf{h}\triangleq[\mathbf{h}_1^T,\cdots,\mathbf{h}_N^T]^T\in\mathbb{R}^{2N\times1}$. Then we can replace constraint (18c) with $\mathbf{q}=\mathbf{h},\mathbf{h}_n\in\mathcal{H},\forall n$, where

$$\mathcal{H}\triangleq\{\,\mathbf{h}_n\mid Q_j^2\le\left\|\mathbf{q}^r[n]-\mathbf{q}_{\mathrm{NF}}^j\right\|^2+2\left(\mathbf{q}^r[n]-\mathbf{q}_{\mathrm{NF}}^j\right)^T\times\left(\mathbf{h}_n-\mathbf{q}^r[n]\right),\quad\forall j\,\} \tag{21}$$

is the feasible region of $\mathbf{h}_n$. In order to improve the convergence rate of ADMM, we use $\mathbf{B}\mathbf{q}-\mathbf{u}=\mathbf{c},\mathbf{c}_n\in\mathcal{C}$, $\forall n$, to express the UAV mobility constraints including the maximum speed constraints in (1a)-(1c) and NFZ constraints in (18c), where $\mathbf{B}\triangleq\left[\mathbf{D}^T,\mathbf{I}_{2N}\right]^T$, $\mathbf{u}\triangleq\left[\mathbf{v}^T,\mathbf{0}_{2N}^T\right]^T$, $\mathbf{c}\triangleq\left[\mathbf{z}^T,\mathbf{h}^T\right]^T$ and $\mathcal{C}\triangleq\{\mathbf{c}_n|\mathbf{c}_n\in\mathcal{Z},n=1,\ldots,N+1,\mathbf{c}_n\in\mathcal{H},n=N+2,\ldots,2N+1\}$ is the feasible region of $\mathbf{c}_n$. Then, problem (19) can be rewritten into the following form

$$\min_{\mathbf{q},\mathbf{t},\mathbf{m},\mathbf{c}} \frac{1}{N}\sum_{n=1}^{N}\Bigg[A^r[n]\|\mathbf{m}[n]-\mathbf{w}_{\mathrm{D}}\|^2 + \log_2\left(1+\frac{\gamma[n]}{t[n]}\right)\Bigg] \tag{22a}$$

$$\text{s.t. } \mathbf{m}=\mathbf{q}, \tag{22b}$$

$$(\mathbf{m},\mathbf{t})\in\mathcal{S}, \tag{22c}$$

$$\mathbf{B}\mathbf{q}-\mathbf{u}=\mathbf{c},\ \mathbf{c}_n\in\mathcal{C},\quad\forall n. \tag{22d}$$

It is observed that problem (22) admits a form of standard global consensus problem which is conducive to the application of ADMM. To apply the ADMM method, we first write the augmented Lagrangian (using the scaled dual variable) of problem (22) as

$$\begin{aligned}&\mathcal{L}(\mathbf{q},\mathbf{t},\mathbf{m},\mathbf{c},\boldsymbol{\beta},\mathbf{y})\\&=\frac{1}{N}\sum_{n=1}^{N}\left[A^r[n]\|\mathbf{m}[n]-\mathbf{w}_{\mathrm{D}}\|^2+\log_2\left(1+\frac{\gamma[n]}{t[n]}\right)\right]\\&\quad+\frac{\rho_1}{2}\|\mathbf{q}-\mathbf{m}+\boldsymbol{\beta}\|^2+\frac{\rho_2}{2}\|\mathbf{B}\mathbf{q}-\mathbf{u}-\mathbf{c}+\mathbf{y}\|^2,\end{aligned} \tag{23}$$

where $\boldsymbol{\beta}$ and $\mathbf{y}$ are the scaled dual variables for constraints (22b) and (22d), respectively. Two different penalty parameters ρ_1 and ρ_2 are adopted to maintain the balance among the penalty term $\|\mathbf{q}-\mathbf{m}+\boldsymbol{\beta}\|^2$ and $\|\mathbf{B}\mathbf{q}-\mathbf{u}-\mathbf{c}+\mathbf{y}\|^2$. According to [29, Sec. 3.4.1], the convergence rate of ADMM algorithm can be improved by adjusting the penalty parameters to keep the above two residual norms within a factor of one another as they both converge to zero.

The general idea of the ADMM is to use the Gauss-Seidel method to update the primal variables, the duplicated variables, and the Lagrange multipliers [29]. The key observation from problem (22) is that the primal variables and the duplicated variables in the constraints can be divided into two blocks, $\{\mathbf{q},\mathbf{c}\}$ and $\{\mathbf{m},\mathbf{t}\}$. Consequently, by alternately updating the three blocks of variables, $\{\mathbf{q},\mathbf{c}\}$, $\{\mathbf{m},\mathbf{t}\}$ and $\{\boldsymbol{\beta},\mathbf{y}\}$, in each iteration as follows, we can obtain decreasing $\mathcal{L}(\mathbf{q},\mathbf{t},\mathbf{m},\mathbf{c},\boldsymbol{\beta},\mathbf{y})$.

a: UPDATING $\{\mathbf{q},\mathbf{c}\}$

The optimization of $\{\mathbf{q},\mathbf{c}\}$ is separable among $\mathbf{q}$ and $\mathbf{c}$, and thus we can update them in a sequential fashion

$$\mathbf{q}^{l+1}=\arg\min_{\mathbf{q}}\frac{\rho_1}{2}\|\mathbf{q}-\mathbf{m}^l+\boldsymbol{\beta}^l\|^2+\frac{\rho_2}{2}\|\mathbf{B}\mathbf{q}-\mathbf{u}-\mathbf{c}^l+\mathbf{y}^l\|^2, \tag{24a}$$

$$\mathbf{c}^{l+1}=\arg\min_{\mathbf{c}}\|\mathbf{B}\mathbf{q}^{l+1}-\mathbf{u}-\mathbf{c}+\mathbf{y}^l\|^2, \tag{24b}$$

with closed form solution of (24a) given by

$$\mathbf{q}^{l+1}=\left(\rho_1\mathbf{I}_{2N}+\rho_2\mathbf{B}^T\mathbf{B}\right)^{-1}\left[\rho_1\left(\mathbf{m}^l-\boldsymbol{\beta}^l\right)+\mathbf{B}^T\left(\mathbf{u}+\mathbf{c}^l-\mathbf{y}^l\right)\right]. \tag{25}$$

As previously defined, the variable $\mathbf{c}$ is the combination of variable $\mathbf{z}$ relating to the maximum speed constraints in (1a)-(1c) and variable $\mathbf{h}$ associated with the NFZ constraints in (18c). Correspondingly, the scaled dual variable $\mathbf{y}$ can be divided into two parts, $\mathbf{y}_1$ for the former constraints and $\mathbf{y}_2$ for the latter one. Therefore, the update of variable $\mathbf{c}$ can be decomposed into two independent problems, one for each of the two sets $\mathbf{z}$ and $\mathbf{h}$, which are given in (26a) and (26b), respectively,

$$\mathbf{z}^{l+1}=\arg\min_{\mathbf{z}_n\in\mathcal{Z}}\|\mathbf{D}\mathbf{q}^{l+1}-\mathbf{v}-\mathbf{z}+\mathbf{y}_1^l\|^2, \tag{26a}$$

$$\mathbf{h}^{l+1}=\arg\min_{\mathbf{h}_n\in\mathcal{H}}\|\mathbf{q}^{l+1}-\mathbf{h}+\mathbf{y}_2^l\|^2. \tag{26b}$$

We note that problem (26a) can be decomposed into $N+1$ independent subproblems, each of which is a convex quadratically constrained quadratic programming (QCQP) with only one constraint (QCQP-1). The processing of problem (26b) resembles (26a). In various cases, QCQP-1 problem can be solved efficiently [40]. In our context, the optimal solutions of (26a) and (26b) can be obtained respectively in closed forms given by

$$\mathbf{z}_n^{l+1} = \begin{cases} \mathcal{L}_{\mathcal{Z}}\left(\mathbf{q}^{l+1}[1] - \mathbf{q}_0 + \mathbf{y}_1^l[1]\right) & n = 1, \\ \mathcal{L}_{\mathcal{Z}}\left(\mathbf{q}^{l+1}[n] - \mathbf{q}^{l+1}[n-1] \right. & \\ \quad \left. + \mathbf{y}_1^l[n]\right) & n = 2, \cdots, N, \\ \mathcal{L}_{\mathcal{Z}}\left(\mathbf{q}_{\mathrm{F}} - \mathbf{q}^{l+1}[N] + \mathbf{y}_1^l[N]\right) & n = N+1, \end{cases} \tag{27a}$$

$$\mathbf{h}_n^{l+1} = \mathbf{q}^{l+1}[n] + \mathbf{y}_2^l[n] + \sum_{j=1}^{J} \theta_{n,j}\left(\mathbf{q}^r[n] - \mathbf{q}_{\mathrm{NF}}^j\right), \quad \forall n, \tag{27b}$$

where $\mathcal{L}_{\mathcal{Z}}\{\mathbf{x}\} \triangleq \min\{\frac{S_{\max}}{\|\mathbf{x}\|}, 1\}\mathbf{x}$ denotes the projector associated with the linear space $\mathcal{Z}$, and $\theta_{n,j}$ denotes the dual variable associated with constraint $\mathbf{h}_n \in \mathcal{H}$, which can be solved by the ellipsoid method. Since the sparsely distributed NFZs are non-overlapped, we can obtain a suboptimal solution of $\mathbf{h}_n^{l+1}$ in a more time-efficient way. If $\mathbf{q}^{l+1}[n] + \mathbf{y}_2^l[n]$ is not in any NFZ, we have $\mathbf{h}_n^{l+1} = \mathbf{q}^{l+1}[n] + \mathbf{y}_2^l[n]$. Otherwise, $\mathbf{q}^{l+1}[n] + \mathbf{y}_2^l[n]$ is in at most one NFZ, which we mark as the k-th one. Then we have $\mathbf{h}_n^{l+1} = \mathbf{q}^{l+1}[n] + \mathbf{y}_2^l[n] + \theta_{n,k}\mathbf{q}_{n,k}^r$, where $\mathbf{q}_{n,k}^r \triangleq \mathbf{q}^r[n] - \mathbf{q}_{\mathrm{NF}}^k$, and $\theta_{n,k}$ is the dual variable relating to the k-th NFZ constraint, which can be decided by

$$g\left(\theta_{n,k}\right) = \mathbf{Q}_k^2 - \|\mathbf{q}_{n,k}^r\|^2 - 2\mathbf{q}_{n,k}^{r^T}\left(\mathbf{q}^{l+1}[n] + \mathbf{y}_2^l[n] + \theta_{n,k}\mathbf{q}_{n,k}^r - \mathbf{q}^r[n]\right). \tag{28}$$

Obviously, there is $\nabla g\left(\theta_{n,k}\right) < 0$. Thus, $g\left(\theta_{n,k}\right)$ is monotonically decreasing in the region $\theta_{n,k} \geq 0$. According to the complementary slackness condition, we have $\theta_{n,k}^* g(\theta_{n,k}^*) = 0$. With the above analysis, we already know $g(0) > 0$. Thus, $g\left(\theta_{n,k}\right)$ has a zero-crossing in the region $\theta_{n,k} > 0$, and we have $g(\theta_{n,k}^*) = 0$. Therefore, closed-form solution of $\theta_{n,k}^*$ can be derived as $\frac{1}{2}\left(\mathbf{q}_{n,k}^{r^T}\mathbf{q}_{n,k}^r\right)^{-1}\Big[\mathbf{Q}_k^2 - \|\mathbf{q}_{n,k}^r\|^2 - 2\mathbf{q}_{n,k}^{r^T}\left(\mathbf{q}^{l+1}[n] + \mathbf{y}_2^l[n] - \mathbf{q}^r[n]\right)\Big]$. Evidently, the solution of $\mathbf{h}_n^{l+1}$ is near the boundary of the k-th NFZ, and would not violate other NFZ constraints due to the sparse distribution of the NFZs.

Based on the analyses above, the optimal solution of (24b) is $\mathbf{c}^{l+1} \triangleq \left[\mathbf{z}^{l+1^T}, \mathbf{h}^{l+1^T}\right]^T$.

b: UPDATING $\{\mathbf{m}, \mathbf{t}\}$

The update of the second block of variables $\{\mathbf{m}, \mathbf{t}\}$ is to solve the following problem

$$\{\mathbf{m}^{l+1}, \mathbf{t}^{l+1}\} = \arg \min_{\{\mathbf{m},\mathbf{t}\}\in\mathcal{S}} \frac{1}{N}\sum_{n=1}^{N}\left[A^r[n]\|\mathbf{m}[n] - \mathbf{w}_{\mathrm{D}}\|^2 + \log_2\left(1 + \frac{\gamma[n]}{t[n]}\right)\right] + \frac{\rho_1}{2}\|\mathbf{q}^{l+1} - \mathbf{m} + \boldsymbol{\beta}^l\|^2. \tag{29}$$

Note that problem (29) can be further decomposed into N QCQP-1 subproblems with closed-form solutions given by

$$\mathbf{m}^{l+1}[n] = \left(2A^r[n] + N\rho_1\right)^{-1}\Big[N\rho_1\left(\mathbf{q}^{l+1}[n] + \boldsymbol{\beta}^l[n]\right) + 2N\mu_n\left(\mathbf{q}^r[n] - \mathbf{w}_{\mathrm{E}}\right) + 2A^r[n]\mathbf{w}_{\mathrm{D}}\Big], \quad \forall n, \tag{30a}$$

$$t^{l+1}[n] = \sqrt{\frac{\gamma^2[n]}{4} + \frac{\gamma[n]\log_2 e}{N\mu_n}} - \frac{\gamma[n]}{2}, \quad \forall n, \tag{30b}$$

where μ_n denotes the dual variable associated with constraint $\{\mathbf{m}, \mathbf{t}\} \in \mathcal{S}$, which can be obtained by applying the bisection method. The details are similar to those in [31], and thus are omitted here.

c: UPDATING LAGRANGE MULTIPLIERS

The last step of the ADMM is to update the Lagrange multipliers as

$$\boldsymbol{\beta}^{l+1} = \boldsymbol{\beta}^l + \mathbf{q}^{l+1} - \mathbf{m}^{l+1}, \tag{31a}$$

$$\mathbf{y}^{l+1} = \mathbf{y}^l + \mathbf{B}\mathbf{q}^{l+1} - \mathbf{u} - \mathbf{c}^{l+1}. \tag{31b}$$

Until now, we have derived the closed-form expressions for all the updating steps at iteration $l+1$.

C. OVERALL ALGORITHM

Due to the non-convexity of the investigated optimization problem (6), there is no general method to obtain the globally optimal solution. Based on the results in previous two subsections, we propose an overall iterative algorithm to obtain a suboptimal solution by applying the AO technique, which solves the two subproblems (7) and (22) alternately in an iterative manner until convergence or the number of iterations rises past $r_{\max}$. The details of the proposed method are shown in Algorithm 1.

1) CONVERGENCE PROOF

We provide the convergence analysis of Algorithm 1 as follows. Firstly, as subproblem (22) is a convex approximate reformulation of the original non-convex subproblem (11), its optimal objective value serves as a lower bound to that of (11). The convergence of the ADMM inner loop in Algorithm 1 is guaranteed according to [29, Sec. 3.2]. Secondly, the objective value achieved by Algorithm 1 is non-decreasing over iterations and upper-bounded by a finite value [14]. As a result, the proposed algorithm is guaranteed to converge at a suboptimal solution for the original problem (6).

2) COMPUTATIONAL COMPLEXITY ANALYSIS

The computational complexity of the proposed algorithm can be analyzed as follows. Recall that N and J denote the number of time slots and NFZs, respectively. We note that in each iteration, the main complexity of Algorithm 1 lies in the operation of the matrix inversion in (25), whose computational cost is $\mathcal{O}(N^3)$. The key observation is that for fixed system parameters, we only need to perform this operation

once in advance, yielding the solution which can be directly used in the ADMM loop. As a result, the complexity of step 5 is about $\mathcal{O}(N^2)$ on the assumption that $J \ll N$. In step 6, the computational cost is $\mathcal{O}(N\log_2\frac{d_n}{\epsilon_n})$, where d_n denotes the length of the original interval of bisection search for μ_n, and ϵ_n represents the given accuracy target, respectively. The complexities of step 7 and 8 are $\mathcal{O}(N^2)$ and $\mathcal{O}(1)$, respectively. Therefore, the total complexity for step 4 to 9 is given by $\mathcal{O}(I^rN^2)$, with I^r denoting the number of iterations needed in the inner loop for solving problem (22) in the r-th iteration. The complexity of step 11 for solving problem (7) is $\mathcal{O}(N)$. Consequently, the total complexity of Algorithm 1 is on the order of $\mathcal{O}(LI^rN^2)$, where L is the number of iterations needed in the outer loop for convergence. Although it is difficult to analyze the growth order of L and I^r with respect to N, simulation results in Section IV show that the proposed algorithm has a great superiority in computational efficiency since each updating step only requires a limited number of multiplications and additions.

3) IMPROVED CONVERGENCE RATE

As mentioned in [30], since only rough estimates of the solution for problem (P1) can be achieved even with completely convergent ADMM inner loop in the first couple of iterations, it would be better to stop the ADMM part after a fixed number of updates (e.g.,I^r_{ADMM}), which would improve the convergence rate of Algorithm 1. The value of I^r_{ADMM} can vary with the evolvement of the outer loop. A little bit different from [30], we set I^r_{ADMM} to be smaller for some first iterations to achieve a good estimate of the solution by the ADMM part. Then, when the outer loop is nearly convergent, we set I^r_{ADMM} to be higher to guarantee the convergence of the ADMM loop such that the optimal solution can meet the mobility constraints.

IV. SIMULATIONS

In this section, numerical results are provided to validate the effectiveness of the proposed algorithm. The legitimate receiver D and eavesdropper E locate at $[0, 0]^T$ and $[200, 0]^T$, respectively. The UAV's maximum flying speed is $V_{\max} = 10$m/s, and the flying altitude is set to $H = 100$m. The horizontal coordinates of the UAV's initial and final locations are respectively set as $\mathbf{q}_0 = [100, 200]^T$ and $\mathbf{q}_{\text{F}} = [100, -200]^T$. Other parameters are as follows: $\delta_t = 0.5$s, $\gamma_0 = 80$dB, $P_{\text{peak}} = 4\bar{P}$, $\epsilon = 10^{-4}$ and $r_{\max} = 30$. The transmit power is initialized as $p^0[n] = \bar{P}, \forall n$, and the initial trajectory adopts the heuristic best-effort manner without NFZ consideration [18]. For illustration, the legitimate receiver D, eavesdropper E, and the UAV's initial and final locations are marked with $\bigcirc$, $\triangle$, $\times$ and $+$.

In the simulations, the performance and complexity of our proposed algorithm (denoted as "ADMM-AO") are compared with the following benchmark methods:

- SCA-AO: the iterative method proposed in [18], but modified slightly to cope with the NFZ constraints. The problem is solved using the CVX package via interior-point solver SDPT3.
- ADMM-NoNFZ: without NFZ consideration during the UAV flight period.
- ADMM-T/NP: trajectory optimization without power control. The transmit power of the UAV in each time slot is set as the average power $\bar{P}$, and the trajectory is optimized by solving the problem (22) iteratively until convergence.

Algorithm 1 ADMM-Based Iterative Algorithm for Solving Problem (P1)

1: Initialize the UAV trajectory $\mathbf{q}^0$, power allocation $\mathbf{p}^0$, $r_{\max}$ and threshold $\epsilon > 0$. Set $r = 0$.
2: **repeat**
3: With given $\{\mathbf{q}^r, \mathbf{p}^r\}$, set the values of $\gamma[n]$ and $A^r[n]$, $\forall n$. Set $l = 0$. Choose feasible initial values for $\left(\mathbf{q}^l, \mathbf{t}^l, \mathbf{m}^l, \mathbf{c}^l, \boldsymbol{\beta}^l, \mathbf{y}^l\right)$ and (ρ_1, ρ_2).
4: **repeat**
5: Update variables $\{\mathbf{q}^{l+1}, \mathbf{c}^{l+1}\}$ by (25) and (27).
6: Update variables $\{\mathbf{m}^{l+1}, \mathbf{t}^{l+1}\}$ by (30).
7: Update variables $\{\boldsymbol{\beta}^{l+1}, \mathbf{y}^{l+1}\}$ by (31).
8: Set $l \leftarrow l + 1$.
9: **until** $l > I^r_{\text{ADMM}}$ or the primal and dual residuals meet the stopping criteria.
10: Set $\mathbf{q}^{r+1} = \mathbf{q}^l$.
11: With given $\mathbf{q}^{r+1}$, update the transmit power allocation $\mathbf{p}^{r+1}$ by (9).
12: Set $r \leftarrow r + 1$.
13: **until** The fractional increase of the objective value is below ϵ.

For all of the above methods, the iteration terminates when the fractional increase of the objective value $\frac{|s^{r+1}-s^r|}{s^r}$ is less than 10^{-4} or a maximum of 30 iterations is reached, where s^r denotes the objective value of the r-th iteration. For the ADMM-based algorithms (namely, ADMM-AO, ADMM-NoNFZ, and ADMM-T/NP), we set $I^r_{\text{ADMM}} = 300$ when the fractional increase is more than 10^{-3}, and $I^r_{\text{ADMM}} = 30000$ for the case that the fractional increase is less than 10^{-3} but more than 10^{-4}. The penalty parameters are set as $\rho_1 = \frac{1}{2500}$, $\rho_2 = \frac{1}{300}$, which are empirically found to converge fast. The stopping criterion of the ADMM is set as recommended in [29, Sec. 3.3] with the absolute tolerance $\epsilon^{\text{abs}} = 10^{-6}$ and the relative tolerance $\epsilon^{\text{rel}} = 10^{-5}$.

A. CONVERGENCE ANALYSIS

We first demonstrate the convergence behavior of the proposed ADMM-AO algorithm for different values of ρ_1 and ρ_2 when $T = 80$s and $\bar{P} = -5$dBm. The algorithm involves an outer-loop iteration for AO and an inner-loop iteration for ADMM, whose convergence properties are illustrated in Fig.2 and Fig.3, respectively. Without loss of generality, we only demonstrate the convergence of the ADMM inner loop for the SCA_1 problem. Here, in Fig.2, the value of

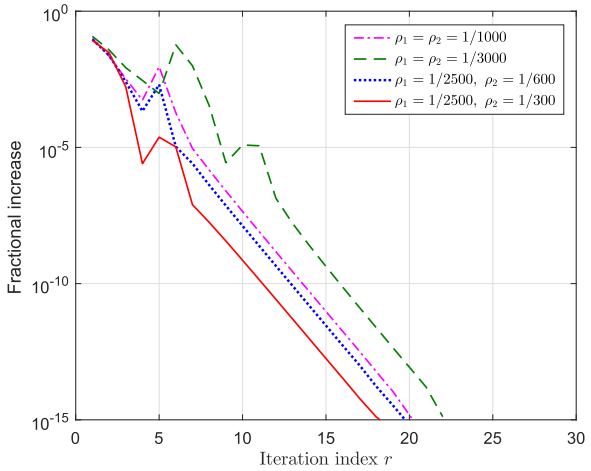


FIGURE 2. Convergence behavior of ADMM-AO algorithm in the outer loop when $T = 80$s and $\bar{P} = -5$dBm.

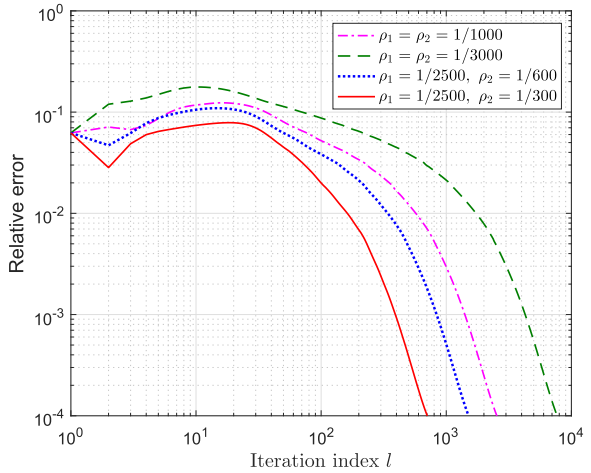


FIGURE 3. Convergence behavior of ADMM-AO algorithm in the inner loop when $T = 80$s and $\bar{P} = -5$dBm.

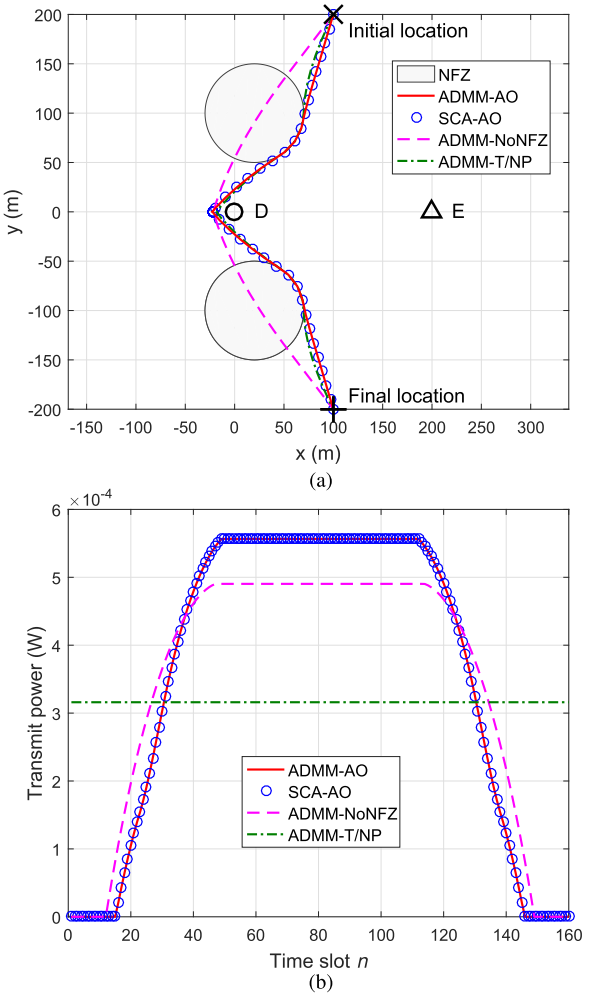


FIGURE 4. Trajectories and transmit power of different algorithms when $T = 80$s and $\bar{P} = -5$dBm. (a) UAV's trajectories. (b) UAV's transmit power.

I^r_{ADMM} follows the aforementioned setting. In Fig.3, the relative error in each iteration is defined as $\frac{|f^l - f^*|}{f^*}$, where f^l is the objective value of the l-th iteration and f^* is the optimal objective value of the given SCA_1 problem. We set the I^1_{ADMM} to be large enough and ignore the stopping criteria to explore the convergence property of the ADMM part. As we can see, the convergence behaviors of ADMM-AO algorithm vary with different values of ρ_1 and ρ_2. From Fig.2, it is observed that the curves fluctuate remarkably in the first stage of iterations because of the incomplete convergence of the ADMM part. Then, with the increasing of iterations, the algorithm achieves a higher convergence accuracy. Fig.3 shows that the setup of $\rho_1 = \frac{1}{2500}$, $\rho_2 = \frac{1}{300}$ significantly improves the convergence speed of the ADMM by compensating for the imbalance between the penalty terms in the Lagrangian function (23). For the remaining simulations, we set $\rho_1 = \frac{1}{2500}$ and $\rho_2 = \frac{1}{300}$, which are empirically found to offer good convergence rate regardless of the values of flight period T and average power $\bar{P}$.

B. TRAJECTORY AND TRANSMIT POWER COMPARISON

Fig.4 shows the trajectories and transmit power of the UAV by applying different algorithms when $T = 80$s and $\bar{P} = -5$dBm. As we can see, the trajectories obtained by ADMM-AO and SCA-AO are almost identical, while that obtained by ADMM-T/NP is much similar to them. If there is no NFZ and T is sufficiently large, as analyzed in [18], the UAV flies at the maximum speed to reach a certain location (not directly above D), then remains stationary there as long as possible, and finally reaches the final location by the end of the last time slot, which is still true when there are NFZs. As illustrated in Fig.4(a), if the optimal path is blocked by the NFZs, our proposed algorithm will find the shortest one tangent to the NFZs. Furthermore, as UAV's transmit power and trajectories are each optimized with the other fixed in an alternating manner, different trajectories will result in different power control. It can be observed from

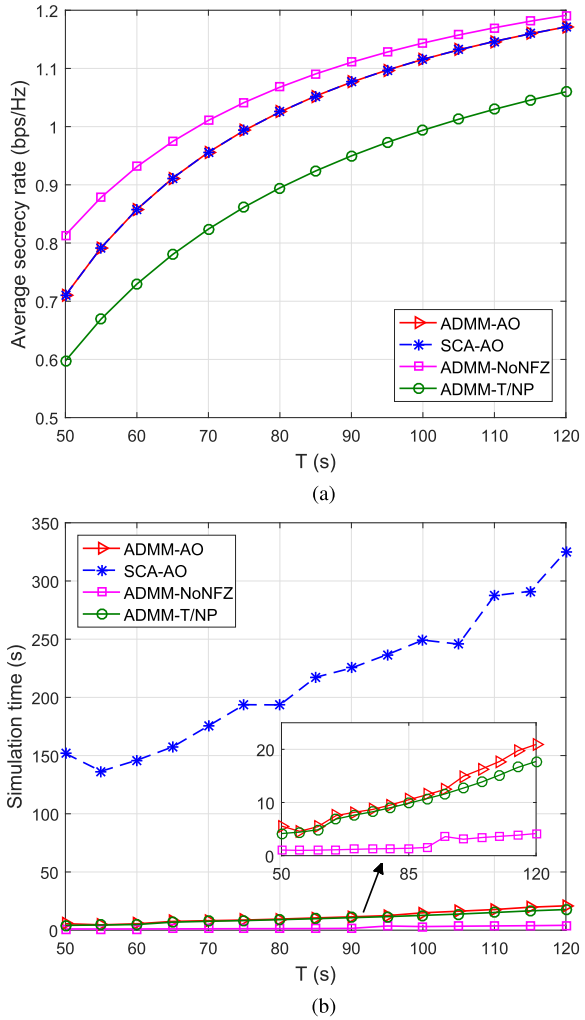


FIGURE 5. (a) Average secrecy rate and (b) simulation time versus flight time T when $\bar{P} = -5$dBm.

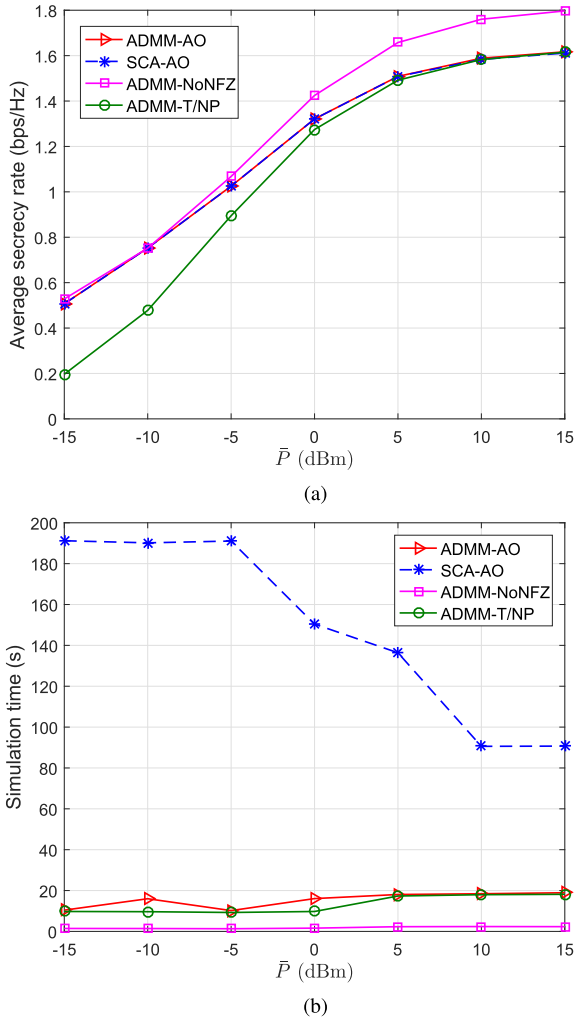


FIGURE 6. (a) Average secrecy rate and (b) simulation time versus average transmit power $\bar{P}$ when $T = 80$s.

Fig.4(b) that the transmit power is closely correlated with the locations of the UAV, which implies the necessity of joint trajectory optimization and power control.

C. PERFORMANCE AND COMPLEXITY COMPARISON

1) COMPARISON WITH VARYING FLIGHT TIME

The average secrecy rates and simulation time of different algorithms versus flight time T are illustrated in Fig.5(a) and Fig.5(b), respectively. Here, the average power is set as $\bar{P} = -5$dBm. From Fig.5(a), it is observed that as T gets larger, the secrecy rates of all schemes strikingly increase, since the UAV can stay longer at the corresponding hovering location for better communication performance. For all simulated periods, ADMM-AO yields almost the same secrecy rates as SCA-AO, both of which remarkably outperform ADMM-T/NP, but underperform ADMM-NoNFZ. Not surprisingly, the existence of the NFZs decrease the average secrecy rates in general. This is mainly because the UAV has to detour to avoid flying over the NFZs, resulting in less hovering time at the stationary location and different power control. However, the average secrecy rates of ADMM-AO and SCA-AO get closer to that of ADMM-NoNFZ as T increases. An explanation might be that since the time for detouring is insignificant compared to the long flight time, the influence of NFZs becomes weaker with increasing T. Moreover, the remarkable rate gap between ADMM-AO and ADMM-T/NP demonstrates that the joint optimization strategy performs better than just trajectory design.

From Fig.5(b), one can see that when the problem size becomes large, the timing curves of all schemes grow visibly. As expected, the three ADMM-based algorithms, namely, ADMM-AO, ADMM-NoNFZ, and ADMM-T/NP, are much more time-saving than the CVX-based SCA-AO method. Although our proposed ADMM-AO performs as well as SCA-AO for all simulated periods, it can speed up the computation time about $15 \sim 30$ times. We also note that the computation time of ADMM-NoNFZ is about $4 \sim 7$ times faster than ADMM-AO and ADMM-T/NP, since extra computation time is needed to deal with the NFZ constraints. Furthermore, as trajectory optimization is more time-consuming than

power control, ADMM-AO only takes a little more time than ADMM-T/NP.

2) COMPARISON WITH VARYING AVERAGE POWER

In Fig.6(a) and Fig.6(b), we illustrate the average secrecy rates and simulation time of different algorithms versus average power $\bar{P}$ when $T = 80$s. Similar observations as in the previous two figures can be observed. As can be seen, the secrecy rates of all schemes increase with $\bar{P}$, and all the rate curves become less steep when $\bar{P}$ is high. Compared with SCA-AO, our proposed ADMM-AO always achieves the same performance, but requires less computation time. Another observation is that the increase in $\bar{P}$ widens the secrecy rate gap between ADMM-NoNFZ and ADMM-AO, due to the fact that the influence of different power control caused by NFZs becomes more significant. On the contrary, although ADMM-AO in general outperforms ADMM-T/NP, the secrecy rate gap between them becomes smaller as $\bar{P}$ increases. This demonstrates that the performance mainly depends on the trajectory optimization when the average transmit power is high.

From Fig.6(b), it can be seen that the increase in $\bar{P}$ leads to the decrease in the computation time of SCA-AO. We also note that the timing curves of ADMM-AO and ADMM-T/NP fluctuate slightly with varying average transmit power $\bar{P}$, since it is difficult to choose the optimal values of penalty parameters ρ_1 and ρ_2 that perform perfectly in all cases.

V. CONCLUSION

This paper has investigated a UAV-enabled secure communication system with the restriction of NFZs as required in some practical scenarios. We have proposed a fast ADMM-based iterative algorithm to maximize the achievable average secrecy rate by jointly optimizing the trajectory and transmit power of the UAV. The algorithm adopts the AO and SCA technique to maintain high-quality performance, and incorporates the ADMM into the SCA framework to realize low-complex implementation. Numerical results verify that our proposed algorithm achieves almost the same performance as the existing CVX-based work, but with substantially reduced computation time. The results of our work can be extended to secure mobile relaying system [21], UAV-aided secure networks with cooperative jamming [23], 3D UAV trajectory design with both altitude and horizontal position optimization, as well as the case with quality-of-service (QoS) guarantees for legitimate receivers, which will be left as future work. Besides, as multiple-antenna techniques are commonly considered in physical layer security for improving secrecy performance [41], an extension of the results in the paper to a scenario with multiple antennas for further security enhancement is worth pursuing in future work. Finally, since the assumption of a single eavesdropper is generally over optimistic, it is worth extending this work to the case with multiple eavesdroppers [19]. However, how to formulate an ADMM form efficiently for this case is challenging and needs further investigation.

REFERENCES

[1] X. Lin *et al.*, "The sky is not the limit: LTE for unmanned aerial vehicles," *IEEE Commun. Mag.*, vol. 56, no. 4, pp. 204–210, Apr. 2018.

[2] A. Al-Hourani, S. Kandeepan, and S. Lardner, "Optimal LAP altitude for maximum coverage," *IEEE Wireless Commun. Lett.*, vol. 3, no. 6, pp. 569–572, Dec. 2014.

[3] R. I. Bor-Yaliniz, A. El-Keyi, and H. Yanikomeroglu, "Efficient 3-D placement of an aerial base station in next generation cellular networks," in *Proc. IEEE Int. Conf. Commun. (ICC)*, May 2016, pp. 1–5.

[4] J. Lyu, Y. Zeng, R. Zhang, and T. J. Lim, "Placement optimization of UAV-mounted mobile base stations," *IEEE Commun. Lett.*, vol. 21, no. 3, pp. 604–607, Mar. 2017.

[5] J. Lyu, Y. Zeng, and R. Zhang, "Cyclical multiple access in UAV-aided communications: A throughput-delay tradeoff," *IEEE Wireless Commun. Lett.*, vol. 5, no. 6, pp. 600–603, Dec. 2016.

[6] Q. Wu, Y. Zeng, and R. Zhang, "Joint trajectory and communication design for UAV-enabled multiple access," in *Proc. IEEE Global Commun. Conf.*, Dec. 2017, pp. 1–6.

[7] Q. Wu and R. Zhang, "Common throughput maximization in UAV-enabled OFDMA systems with delay consideration," *IEEE Trans. Wireless Commun.*, vol. 66, no. 12, pp. 6614–6627, Dec. 2018.

[8] M. F. Sohail, C. Y. Leow, and S. Won, "Non-orthogonal multiple access for unmanned aerial vehicle assisted communication," *IEEE Access*, vol. 6, pp. 22716–22727, 2018.

[9] Q. Wu, J. Xu, and R. Zhang, "Capacity characterization of UAV-enabled two-user broadcast channel," *IEEE J. Sel. Areas Commun.*, vol. 36, no. 9, pp. 1955–1971, Sep. 2018.

[10] Y. Zeng *et al.*, "Throughput maximization for UAV-enabled mobile relaying systems," *IEEE Trans. Commun.*, vol. 64, no. 12, pp. 4983–4996, Dec. 2016.

[11] S. Zhang, H. Zhang, Q. He, K. Bian, and L. Song, "Joint trajectory and power optimization for UAV relay networks," *IEEE Commun. Lett.*, vol. 22, no. 1, pp. 161–164, Jan. 2018.

[12] Y. Zeng and R. Zhang, "Energy-efficient UAV communication with trajectory optimization," *IEEE Trans. Wireless Commun.*, vol. 16, no. 6, pp. 3747–3760, Jun. 2017.

[13] C. Zhan, Y. Zeng, and R. Zhang, "Energy-efficient data collection in UAV enabled wireless sensor network," *IEEE Wireless Commun. Lett.*, vol. 7, no. 3, pp. 328–331, Jun. 2018.

[14] Q. Wu, Y. Zeng, and R. Zhang, "Joint trajectory and communication design for multi-UAV enabled wireless networks," *IEEE Trans. Wireless Commun.*, vol. 17, no. 3, pp. 2109–2121, Mar. 2018.

[15] F. Zhou, Y. Wu, R. Q. Hu, and Y. Qian, "Computation rate maximization in uav-enabled wireless-powered mobile-edge computing systems," *IEEE J. Sel. Areas Commun.*, vol. 36, no. 9, pp. 1927–1941, Sep. 2018.

[16] S. Jeong, O. Simeone, and J. Kang, "Mobile edge computing via a UAV-mounted cloudlet: Optimization of bit allocation and path planning," *IEEE Trans. Veh. Technol.*, vol. 67, no. 3, pp. 2049–2063, Mar. 2018.

[17] Q. Hu, Y. Cai, G. Yu, Z. Qin, M. Zhao, and G. Y. Li, "Joint offloading and trajectory design for uav-enabled mobile edge computing systems," *IEEE Internet Things J.*, to be published. doi: 10.1109/JIOT.2018.2878876.

[18] G. Zhang, Q. Wu, M. Cui, and R. Zhang, "Securing UAV communications via joint trajectory and power control," *IEEE Trans. Wireless Commun.*, vol. 18, no. 2, pp. 1376–1389, Feb. 2019.

[19] M. Cui, G. Zhang, Q. Wu, and D. W. K. Ng, "Robust trajectory and transmit power design for secure UAV communications," *IEEE Trans. Veh. Technol.*, vol. 67, no. 9, pp. 9042–9046, Sep. 2018.

[20] Q. Wang, Z. Chen, W. Mei, and J. Fang, "Improving physical layer security using UAV-enabled mobile relaying," *IEEE Wireless Commun. Lett.*, vol. 6, no. 3, pp. 310–313, Jun. 2017.

[21] Q. Wang, Z. Chen, H. Li, and S. Li, "Joint power and trajectory design for physical-layer secrecy in the UAV-aided mobile relaying system," *IEEE Access*, vol. 6, pp. 62849–62855, 2018.

[22] A. Li, Q. Wu, and R. Zhang, "UAV-enabled cooperative jamming for improving secrecy of ground wiretap channel," *IEEE Wireless Commun. Lett.*, vol. 8, no. 1, pp. 181–184, Feb. 2019. doi: 10.1109/LWC.2018.2865774.

[23] H. Lee, S. Eom, J. Park, and I. Lee, "UAV-aided secure communications with cooperative jamming," *IEEE Trans. Veh. Commun.*, vol. 67, no. 10, pp. 9385–9392, Oct. 2018.

[24] X. Zhou, Q. Wu, S. Yan, F. Shu, and J. Li, "UAV-enabled secure communications: Joint trajectory and transmit power optimization," *IEEE Trans. Veh. Technol.*, to be published. doi: 10.1109/TVT.2019.2900157.

[25] C. Zhong, J. Yao, and J. Xu, "Secure UAV communication with cooperative jamming and trajectory control," *IEEE Commun. Lett.*, vol. 23, no. 2, pp. 286–289, Feb. 2019. doi: 10.1109/LCOMM.2018.2889062.
[26] F. Cheng, G. Gui, N. Zhao, Y. Chen, J. Tang, and H. Sari, "UAV relaying assisted secure transmission with caching," *IEEE Trans. Commun.*, to be published. doi: 10.1109/TCOMM.2019.2895088.
[27] Y. Cai, Z. Wei, R. Li, D. W. K. Ng, and J. Yuan. (2019). "Energy-efficient resource allocation for secure UAV communication systems." [Online]. Available: https://arxiv.org/abs/1901.09308
[28] S. Boyd and L. Vandenberghe, *Convex Optimization*. Cambridge, U.K.: Cambridge Univ. Press, 2004.
[29] S. Boyd, N. Parikh, E. Chu, B. Peleato, and J. Eckstein, "Distributed optimization and statistical learning via the alternating direction method of multipliers," *Found. Trends Mach. Learn.*, vol. 3, no. 1, pp. 1–122, Jan. 2011.
[30] K.-G. Nguyen, Q.-D. Vu, M. Juntti, and L.-N. Tran, "Distributed solutions for energy efficiency fairness in multicell MISO downlink," *IEEE Trans. Wireless Commun.*, vol. 16, no. 9, pp. 6232–6247, Sep. 2017.
[31] E. Chen and M. Tao, "ADMM-based fast algorithm for multi-group multicast beamforming in large-scale wireless systems," *IEEE Trans. Commun.*, vol. 65, no. 6, pp. 2685–2698, Jun. 2017.
[32] Z. Cai, H. Zhou, J. Zhao, K. Wu, and Y. Wang, "Formation control of multiple unmanned aerial vehicles by event-triggered distributed model predictive control," *IEEE Access*, vol. 6, pp. 55614–55627, 2018.
[33] V. Roberge, M. Tarbouchi, and G. Labonté, "Fast genetic algorithm path planner for fixed-wing military UAV using GPU," *IEEE Trans. Aerosp. Electron. Syst.*, vol. 54, no. 5, pp. 2105–2117, Oct. 2018.
[34] R. Li *et al.*, "Joint trajectory and resource allocation design for UAV communication systems," in *Proc. IEEE Globecom Workshops (GC Wkshps)*, Dec. 2018, pp. 1–6.
[35] Q. Wu and R. Zhang, "Delay-constrained throughput maximization in UAV-enabled OFDM systems," in *Proc. 23rd Asia–Pacific Conf. Commun. (APCC)*, Dec. 2017, pp. 1–6.
[36] B. Van Der Bergh, A. Chiumento, and S. Pollin, "LTE in the sky: Trading off propagation benefits with interference costs for aerial nodes," *IEEE Commun. Mag.*, vol. 54, no. 5, pp. 44–50, May 2016.
[37] R. Sun, D. W. Matolak, and W. Rayess, "Air-ground channel characterization for unmanned aircraft systems—Part IV: Airframe shadowing," *IEEE Trans. Veh. Technol.*, vol. 66, no. 9, pp. 7643–7652, Sep. 2017.
[38] P. K. Gopala, L. Lai, and H. El Gamal, "On the secrecy capacity of fading channels," *IEEE Trans. Inf. Theory*, vol. 54, no. 10, pp. 4687–4698, Oct. 2008.
[39] K.-Y. Wang, A. Man-Cho So, T.-H. Chang, W.-K. Ma, and C.-Y. Chi, "Outage constrained robust transmit optimization for multiuser MISO downlinks: Tractable approximations by conic optimization," *IEEE Trans. Signal Process.*, vol. 62, no. 21, pp. 5690–5705, Nov. 2014.
[40] K. Huang and N. D. Sidiropoulos, "Consensus-ADMM for general quadratically constrained quadratic programming," *IEEE Trans. Signal Process.*, vol. 64, no. 20, pp. 5297–5310, Oct. 2016.
[41] X. Chen, D. W. K. Ng, W. Gerstacker, and H. H. Chen, "A survey on multiple-antenna techniques for physical layer security," *IEEE Commun. Surveys Tuts.*, vol. 19, no. 2, pp. 1027–1053, 2nd Quart., 2016.



YING GAO received the B.Eng. degree from the Nanjing University of Science and Technology (NUST), China, in 2016. She is currently pursuing the Ph.D. degree with the Shanghai Institute of Microsystem and Information Technology, Chinese Academy of Sciences, Shanghai, China. Her current research interest includes unmanned aerial vehicle (UAV) communications.



HONGYING TANG received the Ph.D. degree from Shanghai Jiao Tong University (SJTU), China, in 2015. She is currently an Engineer with the Science and Technology on Microsystem Laboratory, Shanghai Institute of Microsystem and Information Technology, Chinese Academy of Sciences. Her research interest includes unmanned aerial vehicle (UAV) communications.



BAOQING LI received the Ph.D. degree from the State Key Laboratory of Transducer Technology, Shanghai Institute of Metallurgy, Chinese Academy of Sciences, Shanghai, China, in 2000. He is currently a Professor and a Ph.D. Supervisor with the Shanghai Institute of Microsystem and Information Technology, Chinese Academy of Sciences. His research interest includes the application of wireless sensor networks.



XIAOBING YUAN received the Ph.D. degree from the Changchun Institute of Optics, Fine Mechanics, and Physics, Chinese Academy of Sciences, Changchun, China, in 2000. He is currently a Professor and a Ph.D. Supervisor with the Shanghai Institute of Microsystem and Information Technology, Chinese Academy of Sciences. His research interests include wireless sensor networks, information transmission, and processing.